7-21-2008

Stimulated Brillouin Scattering Continuous Wave Phase Conjugation in Step-index Fiber Optics

Steven M. Massey

Justin B. Spring

Timothy H. Russell
Air Force Institute of Technology

Recommended Citation

Steven M. Massey, Justin B. Spring, and Timothy H. Russell, "Stimulated Brillouin scattering continuous wave phase conjugation in step-index fiber optics," Opt. Express 16, 10873-10885 (2008). https://doi.org/10.1364/OE.16.010873

Stimulated Brillouin scattering continuous wave phase conjugation in step-index fiber optics

Steven M. Massey*, Justin B. Spring, and Timothy H. Russell

Department of Engineering Physics, Air Force Institute of Technology, 2950 Hobson Way, Wright-Patterson AFB, OH 45433, USA

Corresponding author: smassey@afit.edu

Abstract: Continuous wave (CW) stimulated Brillouin scattering (SBS) phase conjugation in step-index optical fibers was studied experimentally and modeled as a function of fiber length. A phase conjugate fidelity over 80% was measured from SBS in a 40 m fiber using a pinhole technique. Fidelity decreases with fiber length, and a fiber with a numerical aperture (NA) of 0.06 was found to generate good phase conjugation fidelity over longer lengths than a fiber with 0.13 NA. Modeling and experiment support previous work showing the maximum interaction length which yields a high fidelity phase conjugate beam is inversely proportional to the fiber NA^2, but find that fidelity remains high over much longer fiber lengths than previous models calculated. Conditions for SBS beam cleanup in step-index fibers are discussed.

OCIS codes: (190.4370) Nonlinear optics: Nonlinear optics, fibers; (190.5890) Nonlinear optics: Scattering, stimulated; (290.5830) Scattering: Scattering, Brillouin.

References and links

1. E. A. Kuzin, M. P. Petrov, and B. E. Davydenko, "Phase conjugation in an optical fibre," Opt. Quantum Electron. **17**, 393-397 (1985).
2. Y. P. Vasil'ev, P. S. Razenshtein, and E. I. Shklovskii, "Stimulated Brillouin scattering mirror in the form of a multimode optical fiber in a four-pass neodymium phosphate glass laser amplifier," Quantum Electron. **15**, 1417-1418 (1985).
3. A. Heuer, C. Hänisch, and R. Menzel, "Low-power phase conjugation based on stimulated Brillouin scattering in fiber amplifiers," Opt. Lett. **28**, 34-36 (2003).
4. H. J. Eichler, J. Kunde, and B. Liu, "Quartz fibre phase conjugators with high fidelity and reflectivity," Opt. Commun. **139**, 327-334 (1997).
5. V. I. Kovalev and R. G. Harrison, "Continuous wave stimulated Brillouin scattering in optical fibers: new results and applications for high power lasers," Proceedings of SPIE **5975**, 59750L (2006).
6. A. Mocofanescu and K. D. Shaw, "Stimulated Brillouin scattering phase conjugating properties of long multimode optical fibers," Opt. Commun. **266**, 307-316 (2006).
7. L. Lombard, A. Brignon, J. P. Huignard, E. Lallier, and P. Georges, "Beam cleanup in a self-aligned gradient-index Brillouin cavity for high-power multimode fiber amplifiers," Opt. Lett. **31**, 158-160 (2006).
8. B. C. Rodgers, T. H. Russell, and W. B. Roh, "Laser beam combining and cleanup by stimulated Brillouin scattering in a multimode optical fiber," Opt. Lett. **24**, 1124-1126 (1999).
9. T. Russell, W. Roh, and J. Marciante, "Incoherent beam combining using stimulated Brillouin scattering in multimode fibers," Opt. Express **8**, 246-254 (2001).
10. T. H. Russell, B. W. Grime, T. G. Alley, and W. B. Roh, "Stimulated Brillouin scattering beam cleanup and combining in optical fiber," in *Nonlinear Optics and Applications*, H. A. Abdeldayem and D. O. Frazier, ed. (Research Signpost, Kerala, India, 2007), pp. 179-206.
11. R. H. Lehmberg, "Numerical study of phase conjugation in stimulated Brillouin scattering from an optical waveguide," (NRL-MR-4985, Naval Research Lab., Washington, DC (USA), 1982).
12. B. Y. Zel'dovich, V.V. Shkunov, Sov. J. Quantum Electron. **4**, 610–615 (1977).
13. R. W. Hellwarth, "Theory of phase conjugation by stimulated scattering in a waveguide," J. Opt. Soc. Am. **68**, 1050 (1978).
14. G. P. Agrawal, *Nonlinear Fiber Optics* (Academic Press, 2001).
15. J. Spring, "Modeling of SBS Phase Conjugation in Multimode Step Index Fibers," in *Dept of Engineering Physics* (Air Force Institute of Technology, Air University, 2008), pp. 40-89.

#94567 - $15.00 USD Received 1 Apr 2008; revised 20 Jun 2008; accepted 22 Jun 2008; published 7 Jul 2008

16. R. W. Boyd, *Nonlinear Optics* (Academic Press, 2003).
17. H. Bruesselbach, "Beam cleanup using stimulated Brillouin scattering in multimode fibers," in *Conference on Lasers and Electro-Optics* (OSA, 1993), pp. 424-426.
18. D. Gloge, "Weakly guiding fibers," Appl. Opt. **10**, 2252-2258 (1971).
19. M. Gower, and D. Proch, *Optical Phase Conjugation* (Springer, 1994).
20. R. G. Smith, "Optical power handling capacity of low loss optical fibers as determined by stimulated Raman and Brillouin scattering," Appl. Opt. **11**, 2489-2494 (1972).
21. I. 11146-1, "Lasers and laser-related equipment - Test methods for laser beam widths, divergence angles, and beam propagation ratios - Part 1: Stigmatic and simple astigmatic beams," (International Organization for Standardization, 2005).
22. S. Meister, T. Riesbeck, and H. J. Eichler, "Glass fibers for stimulated Brillouin scattering and phase conjugation," Laser and Particle Beams **25**, 15-21 (2007).
23. V. I. Kovalev and R. G. Harrison, "Suppression of stimulated Brillouin scattering in high-power single-frequency fiber amplifiers," Opt. Lett. **31**, 161-163 (2006).

1. Introduction

Fiber optic waveguides provide a long interaction length which lowers the threshold of SBS to power levels easily achievable by CW laser sources. Since the Stokes wave experiences a small Doppler shift, the longitudinal propagation constants of the modes excited by the Stokes wave differ slightly from those excited by the pump. The SBS reflection becomes out of phase with a theoretical perfect phase conjugate reflection over many meters of fiber. As a result, the fidelity of phase conjugation from SBS in step-index fibers decreases with increasing fiber length. While longer fibers are preferred in order to reach threshold at a lower power, shorter fibers are needed to generate a high fidelity phase conjugate beam.

CW phase conjugation in step-index fibers has not been achieved prior to this work. In experiments using pulsed laser sources, there are some instances of fiber lengths longer than a couple meters generating good phase conjugation. Kuzin *et al.* compared phase conjugation characteristics from 7 m and 130 m fibers. While the 7 m fiber produced conjugation better than ~80%, they noted that ~50% depolarization occurred in the Stokes beam for the 130 m fiber[1]. Vasil'ev *et al.* employed a 25 m fiber as a phase conjugate mirror to effectively remove amplifier-induced aberrations[2]. Fiber amplifiers up to 10 m in length have been used as well to generate high fidelity SBS phase conjugation with pulsed lasers pumps[3]. Complicating these results, Eichler *et al.* discovered that the coherence length of the pump laser limited the interaction length in SBS phase conjugation experiments[4]. Even though they used fibers as long as 100 m to generate high fidelity phase conjugation, the effective length of the interaction was limited to a few meters by the coherence length of the pump laser.

Long graded-index fibers have been reported to produce CW phase conjugation[5, 6], but other researchers have been unable to duplicate the results[7-9]. Both modeling and experimental work in graded index fibers has shown that preferential Stokes gain in the fundamental mode can inhibit phase conjugation fidelity and lead to an effect known as SBS beam cleanup[10].

In order to design efficient CW laser systems using SBS phase conjugation for coherent beam combination, the length of fiber that can be used to generate a high fidelity phase conjugate reflection must be explored further. In this paper, the phase conjugate fidelity is measured as a function of fiber length during cutback tests on two different silicate step-index fibers. Fidelity was lower at longer lengths of fiber. As the fibers were cut back, the fidelity increased to ~80% at 40 m of a 40 μm core diameter, 0.06 NA fiber (CorActive Ge740). Similar fidelity was achieved from 15 m of 20 μm core, 0.13 NA fiber (CorActive MM-20/125). In this work, the two fibers are related based on the fidelity obtained as a function of fiber length when scaled by the square of the fiber core NA. The experimental and modeling results show a similar trend in fidelity as a function of fiber length.

#94567 - $15.00 USD Received 1 Apr 2008; revised 20 Jun 2008; accepted 22 Jun 2008; published 7 Jul 2008

2. Experiment

The apparatus is shown in Fig. 1. It consists of a 1064 nm NPRO narrow-linewidth source laser operating at 700 mW and a 2-stage fiber amplifier. The first fiber amplifier is 10.3 m of Nufern's Yb-doped 20/400 PLMA fiber counter-pumped with a 20 W LIMO fiber-coupled diode through a dichroic mirror. The output of the first stage is 5.5 W. The second stage is 5.2 m of the same 20/400 PLMA fiber, co-pumped with a 100 W LIMO fiber-coupled diode. Co-pumping was chosen to prevent damage to the diodes, and the fiber length was reduced to prevent the onset of SBS in the amplifier. The shortened length reduced the pump absorption in the fiber by approximately 20%. The 2-stage amplifier produced an output power of ~50 W.

Free space coupling was used throughout this experiment, and each fiber tip including the test fiber was polished at 8° to prevent cavity effects and Fresnel reflection noise in the data. The output of the first stage amplifier was over 95% linearly polarized. To bypass polarization control on the high power amplifier, each polarization of the signal beam after the second stage amplifier was separately isolated and recombined.

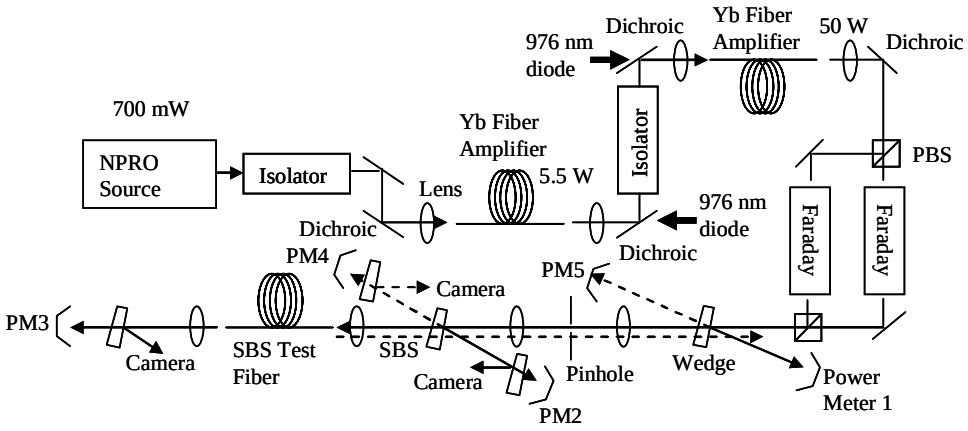

Fig. 1. Apparatus used to test phase conjugation fidelity of silicate fibers at 1064 nm wavelength.

The method employed to measure fidelity is similar to Kuzin *et al.* [1]. The full signal beam is focused through a 300 μm diameter pinhole before propagating to the test fiber. The pinhole is imaged onto the fiber tip such that the pinhole image diameter is less than half of the core diameter of the fiber. The pinhole image size was chosen as small as possible and ultimately limited by the NA of the test fiber to maintain coupling efficiency. The test fiber itself distorts the beam as many modes are excited. Since the incident beam passed through the pinhole, a perfect phase conjugate reflection would have complete transmission back through the pinhole. The pinhole transmission of the Stokes reflection is now a measure of the fidelity of phase conjugation.

This fidelity measurement technique can distinguish between phase conjugation and SBS beam cleanup to the fundamental mode. Since the pinhole has a smaller image diameter than the fundamental fiber mode, it can be calculated that up to 66% pinhole transmission can be achieved in the event that the Stokes reflection propagates in the fundamental mode provided the pinhole image is centered on the fiber tip. Similarly, a flat-top beam should achieve transmission less than 25%. As with all spatial measurements of phase conjugation fidelity, low fidelity measurements are ambiguous.

The test fiber was aligned to maximize transmission through the fiber at low power. Wedged windows with anti-reflection coating on one side were used to measure the power

#94567 - $15.00 USD Received 1 Apr 2008; revised 20 Jun 2008; accepted 22 Jun 2008; published 7 Jul 2008

before and after the pinhole. Additional beam pickoffs were used to reflect portions of the beam to a screen where a Cohu camera simultaneously recorded the beam irradiance cross-section incident on the test fiber, the transmission through the test fiber, and the Stokes reflection.

The fiber was cut back in set intervals, polished, and tested at its new length without disturbing the input end of the test fiber. This enabled the measurement of fidelity as a function of fiber length. To measure fidelity, the power meters labeled PM4 and PM5 in Fig. 1 were connected to an oscilloscope. The powers were measured simultaneously by the oscilloscope and the ratio of PM5 to PM4 provided the raw fidelity data. To calibrate the measurements, an HR mirror was placed in front of the fiber and aligned to reflect the incident beam back through the pinhole towards the amplifiers. The pinhole was then removed, and calibration data consisted of the ratio of PM5/PM4 as a function of the PM4 power. This accounted for differences in the power meters as well as for small losses from each optic between PM4 and PM5. To avoid large errors caused by dividing by voltages near zero, all data corresponding to reflected powers less than 600 mW was discarded. A single data point consists of the average of all calibrated data after SBS threshold is exceeded giving a Stokes reflection greater than 600 mW. Typically, multiple points were taken at each length.

Table 1. SBS test fiber and coupling characteristics

	0.13 NA fiber	0.06 NA fiber
Core diameter (μm)	20	40
Core NA	0.13	0.06
Fiber M^2 (V/2)	3.8	3.5
Fundamental mode $1/e^2$ diameter (μm)*	14.5	29.4
Pinhole image diameter at fiber tip (μm)	9.6	18.5
Incident beam diameter at fiber tip (μm)	5.5+/-0.3	11.3+/-0.6
Coupling NA	0.119+/-0.006	0.057+/-0.004
Coupling efficiency (%)	79+/-5	84+/-5

*Marcuse, D., *Loss analysis of single-mode fiber splices*. Bell Syst. Tech. J, 1977. 56(5): p. 703–718.

The results of the cutback test show a distinct increase in phase conjugation fidelity as each fiber is shortened. 79+/-1% phase conjugation fidelity was achieved with fiber length of 15 m for the 20 μm core, 0.13 NA fiber (Fig. 2). The blue dots with error bars are the experimental results, while the blue line represents modeling results discussed in the next section. The red dashed line represents fidelity as a function of length given by Eq. (1.13) below. With a 40 m long fiber, the fidelity was ~40%. In contrast, a fidelity of 82+/-1% was obtained from a 40 m length of the 0.06 NA, 40 μm core fiber (Fig. 3), which was increased from 65% at 100 m length.

When an HR mirror was placed in front of the fiber, up to 82% of the reflected power would transmit through the pinhole. The deviation from 100% is due to imperfect collimation of the incident beam and diffraction effects. Tests were also conducted with an HR mirror placed after the test fiber to reflect power back through the test fiber and pinhole. The HR mirror was adjusted to maximize transmission back through the test fiber and pinhole. With the 40/400, 0.06 NA fiber, the pinhole transmission of such a reflected beam was between 0% and 57% depending on the fiber modes excited by the reflected signal. With the 20/125, 0.13 NA fiber, the pinhole transmission achieved with an HR mirror after the fiber was between 0% and 43%.

#94567 - $15.00 USD Received 1 Apr 2008; revised 20 Jun 2008; accepted 22 Jun 2008; published 7 Jul 2008

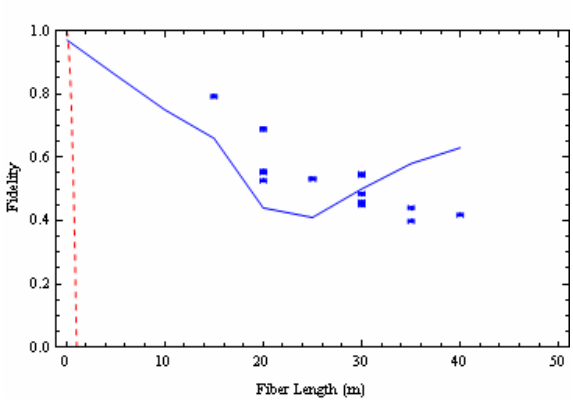

Fig. 2. Phase conjugation fidelity vs. fiber length for a 20 µm core, 0.13 NA silicate fiber. The experimental data is compared to this work's model and Hellwarth's model (red dotted line).

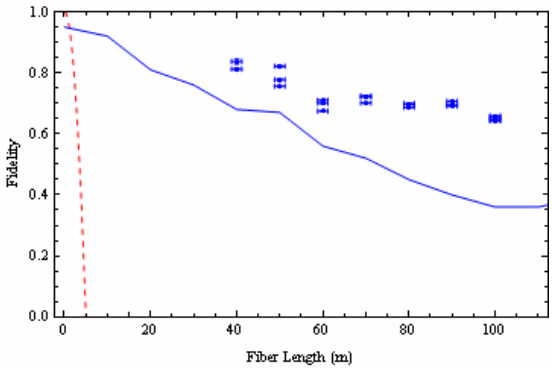

Fig. 3. Phase conjugation fidelity vs. fiber length with a 40 µm core diameter, 0.06 NA fiber. The experimental data is plotted along with the results of this work's model and Hellwarth's model (red dashed line).

Images were taken of the beam incident on the test fiber, the test fiber transmitted beam, and the Stokes reflection from these two fibers. The beams are reflected from wedged windows placed in front of PM2 (incident), PM3 (transmitted), and PM4 (SBS) shown in Fig. 1, and each beam was propagated to a screen and imaged simultaneously. The images are shown in Fig. 4 and Fig. 5 to show general beam shape and relative divergence. In each image, the incident beam is shown in the upper left of the frame, the transmitted beam is in the upper right, and the Stokes beam is shown in the lower portion of the frame.

The transmission through the test fiber is multimode in each image, and the Stokes beam is single-lobed for all lengths tested using the 0.06 NA fiber. Coupling conditions were varied prior to the cutback test and would occasionally result in an LP_{11} Stokes beam using a 100 m length of fiber. While the front of the fiber was not disturbed throughout the cutback tests, the back end had a new 8° polish and slight differences in location after each cut. These changes in the back end of the test fiber caused the beam to move relative to the camera image.

For the 0.13 NA fiber, the images show the Stokes beam in the LP_{11} mode at 40 m and a progression toward single mode as the fiber is shortened. The incident beam was coupled 7+/-2 µm off-center, which was the most-likely cause of the LP_{11} mode in the Stokes beam at longer fiber lengths where phase conjugation fidelity declines. As the fiber length was shortened, the phase conjugation fidelity improved and the LP_{11} mode was gradually replaced by a phase conjugate of the incident beam (SBS pump). The model described in the next

#94567 - $15.00 USD Received 1 Apr 2008; revised 20 Jun 2008; accepted 22 Jun 2008; published 7 Jul 2008

section predicts the occurrence of beam cleanup in step-index fibers when the test fiber is too long for good fidelity phase conjugation.

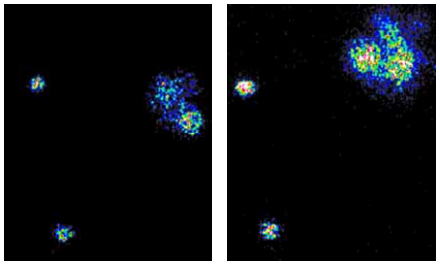

Fig. 4. Clockwise from top left: Incident beam, test fiber transmitted beam, and Stokes reflection from 40/400, 0.06 NA fiber at (a) 100 m length and (b) 40 m length.

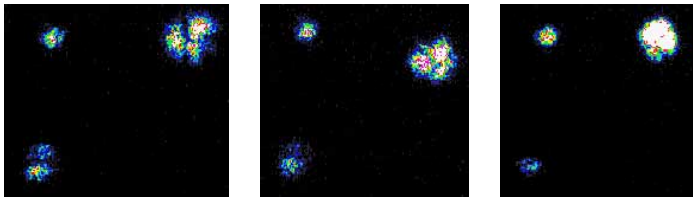

Fig. 5. Clockwise from top left: Incident, transmitted, and Stokes reflection from 20/125, 0.13NA fiber at (a) 40 m length, (b) 30 m, and (c) 15 m length. Without changing the coupling, the Stokes reflection is 2-lobed at 40m length and converts to single transverse mode as the fiber length is decreased.

3. Model

This author is aware of several models of phase conjugation fidelity using SBS in optical waveguides. Each model is accurate for the case of fidelity near 1, but approximations were made which invalidate the models for decreased fidelity. Lombard solved for the gain per mode under the case of perfect phase conjugation or perfect beam cleanup, but does not solve for fidelity[7]. Deviations from the cases of perfect beam cleanup or perfect phase conjugation were not analyzed. Pump depletion was treated uniformly for all modes, which was done similarly in this work, but a functional form was not presented. Lehmberg's numerical model examined the fidelity as a function of average irradiance and divergence angle over short interaction lengths[11]. Lehmberg accounts for pump depletion, but the model sets $\Delta\lambda = 0$ and therefore fails to account for a decrease in fidelity as fiber length is increased. Both Zel'dovich and Shkunov[12] and Hellwarth[13] reach analytical solutions for the length limitation on fidelity by neglecting pump depletion and solving for the case of near perfect fidelity. Zel'dovich approximates the non-conjugated fraction of the Stokes beam in Taylor series expansion and keeps only the first few terms, which limits the validity of the model to near perfect fidelity[12]. This method resulted in an equation dependent on pump irradiance pattern. Hellwarth evaluated the phase conjugate fidelity that could be obtained from a waveguide as a function of waveguide length, core area, and number of modes excited. His analysis is based on a perturbation of perfect fidelity phase conjugation which loses validity as fidelity decreases. Russell *et al.* analyzed the phase difference accumulated between the lowest and highest order modes supported by the fiber to determine the maximum fiber length allowed by a given phase difference accumulated between the Stokes and pump modes[10]. This model clearly shows an increasing phase error as the length of fiber is

#94567 - $15.00 USD Received 1 Apr 2008; revised 20 Jun 2008; accepted 22 Jun 2008; published 7 Jul 2008

increased, but the relationship between phase mismatch and phase conjugation fidelity is undetermined.

The model described here is a three-dimensional analysis of phase conjugation in step-index waveguides which includes pump depletion effects. Free-space Fourier propagation was used to propagate a Gaussian beam through a pinhole and focus off-center onto the tip of a fiber as done in the experiment. The fiber modes were determined from its physical characteristics with numerical root solving methods to find the modal transverse and longitudinal propagation constants. The electric field of each mode in a transverse plane was then determined from the propagation constants. The product of the incident field and a random field in the fiber was integrated over the transverse dimension at the face of the fiber and maximized using a perturbation algorithm to obtain a set of fiber modes with amplitudes and phases that closely matched the incident field. The SBS portion of the model solves for the Stokes field at the tip of the fiber by perturbing the Stokes field until one is found which experiences the highest SBS gain. The resulting Stokes beam is counterpropagated in free space to determine the transmission through the pinhole. The SBS portion of the model is discussed in more detail here.

The equations describing stimulated Brillouin scattering are given by[14]

$$\begin{aligned}\frac{\partial I_p(r_\perp,z)}{\partial z} &= -g(r_\perp)\frac{\omega_p}{\omega_s}I_p(r_\perp,z)I_s(r_\perp,z)-\alpha_p I_p(r_\perp,z)\\ \frac{\partial I_s(r_\perp,z)}{\partial z} &= -gI_s(r_\perp,z)I_p(r_\perp,z)+\alpha_s I_s(r_\perp,z)\end{aligned} \tag{1.1}$$

where $g(r_\perp)$ represents the Brillouin gain, $I_{p,s}(r_\perp)$ represents the irradiance of the pump or Stokes beam, $r_\perp$ is the transverse fiber direction, and $\alpha_{p,s}$ represents transmission loss in the fiber at the pump and Stokes beam frequency. The transmission loss in silicate fibers is typically less than 5 dB/km and will be neglected due to the relatively short lengths of fiber where this model is concerned. The pump and stokes fields are represented as a summation over the fiber mode fields as[10]

$$E_{p,s}(r_\perp,z,t)=\sum\nolimits_f A^f_{p,s}(r_\perp)\psi^f_{p,s}(r_\perp)\cos(\beta^f_{p,s}z-\omega_{p,s}t+\phi^f_{p,s}) \tag{1.2}$$

The summation is over all the modes allowed by the fiber f, and includes both radial and azimuthal dependence represented by a single variable $r_\perp$. The amplitude of each pump or Stokes mode is represented by $A^f_{p,s}(z)$, and the field radial and azimuthal dependence is given by $\psi^f_{p,s}(r_\perp)$. $\beta^f_{p,s}$ is the longitudinal propagation constant for the particular pump or Stokes mode, while $\omega_{p,s}$ and $\phi^f_{p,s}$ are the pump or Stokes radial frequency and modal phase factor respectively. Following the work of Russell et. al.[10], the irradiance of a pump or Stokes mode is given by

$$\begin{aligned}I_{p,s}(r_\perp,z) &= 2\varepsilon_0 cn\left\langle E_{p,s}(r_\perp,z,t)^2\right\rangle\\ &= \varepsilon_0 cn\sum\nolimits_{f,q}A^f_{p,s}(r_\perp)A^q_{p,s}(r_\perp)\psi^f_{p,s}(r_\perp)\psi^q_{p,s}(r_\perp)\cos(\Delta\beta^{fq}_{p,s}z+\Delta\phi^{fq}_{p,s}),\end{aligned} \tag{1.3}$$

where the brackets indicate a time average of the field, ε_0 is the permittivity of free space, n is the index of refraction of the fiber core, and c is the speed of light. Shorthand notation was used such that $\Delta\beta^{fq}_{p,s}=\beta^f_{p,s}-\beta^q_{p,s}$ and similarly for $\Delta\phi^{fq}_{p,s}$. SBS causes an increase in amplitude of the scattered fields which correspond to a decrease in amplitude of the pump fields. In reality, these rates are mode dependent and coupled together such that the Stokes increase in one mode may correspond to a decreased amplitude of multiple pump modes. To

#94567 - $15.00 USD Received 1 Apr 2008; revised 20 Jun 2008; accepted 22 Jun 2008; published 7 Jul 2008

simplify this analysis, all the modes of either the pump or Stokes are approximated to vary at the same rate. This can be represented by[10]

$$A_{p,s}^{f}(z) = \kappa_{p,s}(z) A_{p,s}^{f}(0) \,. \tag{1.4}$$

In this equation, $\kappa_{p,s}(z)$ represents the change in amplitude common to all modes of either the pump or Stokes beams, and $A_{p,s}^{f}(0)$ represents the mode field amplitude at the pump input end of the fiber. By integrating over the transverse area, the change in Stokes irradiance (Eq. (1.1)) can now be expressed as[10]

$$\frac{\partial P_s(z)}{\partial z} = g(\varepsilon_0 cn)^2 \sum\nolimits_{f,q,j,v} A_{ppss}^{fqjv} \gamma_{ppss}^{fqjv} \kappa_s(z)^2 \kappa_p(z)^2 \cos(\Delta\beta_p^{fq} z + \Delta\phi_p^{fq}) \cos(\Delta\beta_s^{jv} z + \Delta\phi_s^{jv}) \tag{1.5}$$

which includes new notation

$$\begin{aligned} A_{ppss}^{fqjv} &= A_p^f(0) A_p^q(0) A_s^j(0) A_s^v(0) \\ \gamma_{ppss}^{fqjv} &= \int \psi_p^f(r_\perp) \psi_p^q(r_\perp) \psi_s^j(r_\perp) \psi_s^v(r_\perp) dr_\perp \end{aligned} \tag{1.6}$$

After making the substitution $\kappa_s(z)^2 = P_s(z)/P_s(0)$, Eq. (1.5) can be integrated using separation of variables to yield an equation for $P_s(z)$ [15]

$$P_s(z) = \exp\left[-\frac{g(\varepsilon_0 cn)^2}{P_s(0)} \int \sum\nolimits_{f,q,j,v} A_{ppss}^{fqjv} \gamma_{ppss}^{fqjv} \kappa_p(z)^2 \cos(\Delta\beta_p^{fq} z + \Delta\phi_p^{fq}) \cos(\Delta\beta_s^{jv} z + \Delta\phi_s^{jv}) dz \right] \tag{1.7}$$

To evaluate the integral in the exponential, an expression for $\kappa_p(z)$ must be found. The assumption that all the pump modes are depleted at the same rate is equivalent to a single-mode fiber approximation with a constant transverse intensity profile across the core for purposes of pump depletion. The additional approximation that the fiber is lossless has already been discussed, and yields the differential equations

$$\begin{aligned} \frac{\partial I_p(z)}{\partial z} &= -g I_p(z) I_s(z) \\ \frac{\partial I_s(z)}{\partial z} &= -g I_s(z) I_p(z) \end{aligned} \tag{1.8}$$

As discussed by Boyd[16], these equations imply $I_p(z) = I_s(z) + C$ where C is a constant, and recall that $\kappa_p(z)^2 = I_p(z)/I_p(0)$. Separation of variables can then be used to solve Eq. (1.8),

$$\kappa_p(z)^2 = \frac{I_s(0)[I_p(0) - I_s(0)]}{I_p(0)^2 \exp\{gz[I_p(0) - I_s(0)]\} - I_s(0) I_p(0)} + 1 - \frac{I_s(0)}{I_p(0)} \tag{1.9}$$

The procedure detailed by Boyd[16] for the "SBS Generator" was used to solve a transcendental equation for $I_s(0)$ in terms of total SBS gain $G = g I_p(0) L$ and SBS threshold gain as determined by experiment. Using this description of pump depletion, Eq. (1.7) was evaluated numerically.

To reduce computation time, the product of cosines in Eq. (1.7) was approximated as done by Hellwarth [13]. Using the trigonometric identity,

$$\begin{aligned} &2\cos(\Delta\beta_p^{fq} z + \Delta\phi_p^{fq}) \cos(\Delta\beta_s^{jv} z + \Delta\phi_s^{jv}) \\ &= \cos[(\Delta\beta_p^{fq} - \Delta\beta_s^{jv}) z + \Delta\phi_p^{fq} - \Delta\phi_s^{jv}] + \cos[(\Delta\beta_p^{fq} + \Delta\beta_s^{jv}) z + \Delta\phi_p^{fq} + \Delta\phi_s^{jv}] \end{aligned} \tag{1.10}$$

#94567 - $15.00 USD Received 1 Apr 2008; revised 20 Jun 2008; accepted 22 Jun 2008; published 7 Jul 2008

For nonzero $\Delta\beta_p^{fq}$ and $\Delta\beta_s^{jv}$, most mode combinations result in large values for these $\Delta\beta$ terms which oscillate rapidly and integrate to negligible values over short fiber distances. Only certain mode combinations were computed in the model. When $f = q$ and $j = v$, both cosine terms on the right hand side of Eq. (1.10) equal one. Owing to the similarity of the propagation constants under the small frequency shift of SBS, the contribution of the cosine term will be small compared to the case of $f = j$ and $q = v$ for the first cosine term on the right hand side of Eq. (1.10), that is, when the pump and Stokes modes being compared are in corresponding fiber modes. The same is true when $f = v$ and $q = j$ for the second cosine term on the right of the equation. Therefore, the product of cosines is simplified to[15]

$$\cos(\Delta\beta_p^{fq} z + \Delta\phi_p^{fq})\cos(\Delta\beta_s^{jv} z + \Delta\phi_s^{jv}) \simeq \begin{cases} \frac{1}{2}\cos[(\Delta\beta_p^{fq} - \Delta\beta_s^{jv})z + \Delta\phi_p^{fq} - \Delta\phi_s^{jv}], \text{ if } f = j \text{ and } q = v \neq f \\ \frac{1}{2}\cos[(\Delta\beta_p^{fq} + \Delta\beta_s^{jv})z + \Delta\phi_p^{fq} + \Delta\phi_s^{jv}], \text{ if } f = v \text{ and } q = j \neq f \\ 1 \quad , \text{if } f = q \text{ and } j = v \\ 0 \quad , \text{otherwise} \end{cases} \tag{1.11}$$

The Stokes beam generated in the fiber is the combination of fiber modes that experiences the highest SBS gain. For a given combination of Stokes modes, the backscattered Stokes power can be computed using Eqs. (1.11) and (1.9) to solve Eq. (1.7). An algorithm was used to find the amplitudes and phases of the Stokes modes that produced the maximum backscattered power for a given pump configuration. The algorithm steps through the amplitude and phase of each Stokes mode and outputs the solution when the iteration fails to improve power more than a set percentage. The sum of all the Stokes modes is then propagated back through free space to the pinhole aperture to determine fidelity.

4. Discussion

The model and experiment show higher fidelity generated by longer lengths of fiber than previously calculated by approximately an order of magnitude as shown in Fig. 2 and Fig. 3. The fidelity level obtained in the model is typically 10-20% lower than the experimental data as the fidelity decreases from one and levels off at a low fidelity level. The main source of error is the approximation that all pump modes and, separately, all Stokes modes vary equally with power as a function of length.

The form of pump depletion chosen has an impact on the rate of decrease in fidelity with fiber length. Ignoring pump depletion leads to an exponential growth of the Stokes modes in the backward direction. This sharp rise in Stokes power weights the front end of the fiber such that the Stokes modes matching the pump at the front of the fiber receive the highest Brillouin gain regardless of fiber length. Using Eq. (1.9) to describe pump depletion slows the rapid Stokes growth and extends the interaction length to produce a more realistic decay in fidelity as a function of fiber length.

After the fidelity has dropped to a low value, the model predicts a rise in fidelity as the fiber length is increased further which is not apparent in the experimental data. This is an artifact in the model that results when $(\Delta\beta_p^{fq} \pm \Delta\beta_s^{jv})z = m2\pi$, where m is an integer. When multiple mode sets reach an integer number of 2π change in phase near the same length of fiber, the mode mismatch is mitigated and fidelity increases at that length of fiber. However, the experiment failed to confirm this result. The common mode amplitude growth and decay rate used in the model prevents the relative power between modes from evolving along the length of the fiber as occurs in the experiment, which may be responsible for this resonance effect in the model.

#94567 - $15.00 USD Received 1 Apr 2008; revised 20 Jun 2008; accepted 22 Jun 2008; published 7 Jul 2008

The model predicts beam cleanup in step-index fibers longer than the limited length required for good fidelity phase conjugation as observed in Fig. 5 and by Bruesselbach[17]. Instead of a phase conjugate, the Stokes beam may predominantly excite a single fiber mode as the fiber length increases. The mode excited is that which experiences the highest SBS gain and is highly dependent on coupling geometry. Coupling on-axis typically results in beam cleanup to the fundamental mode. An example of beam cleanup to the LP_{11} mode as produced by off-axis coupling is shown modeled in Fig. 6.

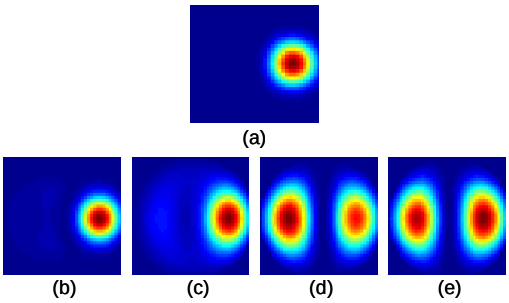

Fig. 6. Model results showing phase conjugation and beam cleanup to the LP_{11} mode in a 20 micron core diameter, 0.13 NA fiber with pump irradiance (a). The resulting Stokes irradiance patterns are shown from a fiber with lengths (b) 1 m, (c) 5 m, (d) 20 m, and (e) 250 m.

The phase conjugation fidelity achieved with the 0.06 NA fiber in both modeling and experiment decreased with length at a much slower rate than the fiber with 0.13 NA. Although the calculations of Zel'dovich and Hellwarth lose validity as the nonconjugated fraction becomes large, both of their models include an analytic solution for the interaction length that is inversely proportional to the NA^2 of the fiber. Specifically, Hellwarth's model resulted in an expected SBS phase conjugation fidelity as a function of fiber length, core area, and the number of modes excited in the fiber:

$$L \le \frac{6\sqrt{(1-F)}A}{N_w \Delta\lambda} \tag{1.12}$$

where F is the phase conjugation fidelity, A is the fiber core area, N_w is the number of modes excited in the fiber, and the Brillouin shift in wavelength is given by $\Delta\lambda$. By approximating the number of modes as $N_w \approx \frac{V^2}{2} = \frac{\left(k_o a\left(NA\right)\right)^2}{2}$ [18], this equation states that the length of fiber that can be used to produce a given phase conjugation fidelity is inversely related to the square of the fiber core numerical aperture[19]:

$$L \le \frac{6\sqrt{(1-F)}c}{NA^2 \Omega_B} \tag{1.13}$$

where the Stokes shift is represented by angular frequency $\Omega_B = 2\pi c \frac{\Delta\lambda}{\lambda^2}$. Similarly, Zel'dovich' model results in a length limitation of

$$L \le \frac{3\sqrt{1-F}Mc}{n\Omega_B NA^2} \tag{1.14}$$

where n is the index of refraction of the core and M is a scalar used to account for the spatial pump irradiance pattern such as Gaussian ($M = 2.8$) or a flat-top beam ($M = 12$). The

#94567 - $15.00 USD Received 1 Apr 2008; revised 20 Jun 2008; accepted 22 Jun 2008; published 7 Jul 2008

models nearly converge in the case of a Gaussian pump. In addition, Russell demonstrated a similar dependence as a function of phase error $\Delta\phi$ [10]

$$L = \frac{2nc\Delta\phi}{\Omega_B NA^2} \tag{1.15}$$

In accordance with these analytic results, the fiber lengths in these experiments were compared based on the physical length of the fiber, the Stokes shift, and the square of the fiber core NA. The scaled length parameter has units of meter·GHz

$$L_s \equiv L\Omega_B NA^2 . \tag{1.16}$$

According to Eq. (1.13), (1.14), and (1.15), L_s is a constant for a given phase conjugate fidelity. In Fig. 7, the fidelity achieved with the two fibers as a function of fiber length is plotted for both modeling and experimental results in this work. In Fig. 8, these results are plotted against the scaled length parameter, L_s. The data from the model and experiment are well correlated using this relationship. A fidelity of 80+/-2% was achieved experimentally at a scaled length of ~20 m·GHz. Also included in Fig. 8 is the plot of Eq. (1.13).

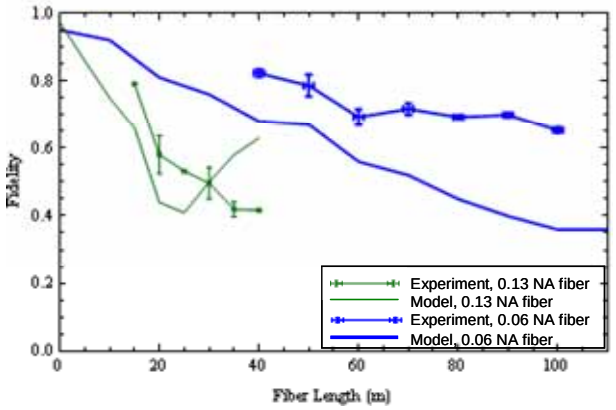

Fig. 7. Fidelity vs. fiber length for the 0.06 NA and 0.13 NA fibers, including both modeling and experiment.

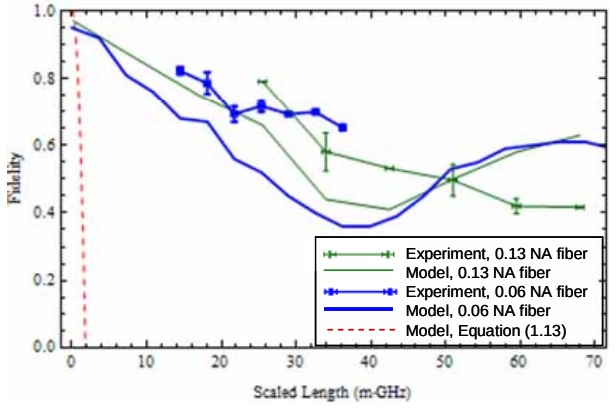

Fig. 8. The fidelity from both modeling and experiment is plotted against a scaled fiber length.

Using the scaled length parameter, the SBS threshold power can be approximated as a function of the quality of the beam to be conjugated. The SBS threshold for a given fiber is approximately given by[20]

#94567 - $15.00 USD Received 1 Apr 2008; revised 20 Jun 2008; accepted 22 Jun 2008; published 7 Jul 2008

$$P_{th} = \frac{21A}{gL} \tag{1.17}$$

Solving Eq. (1.16) for L and substituting into (1.17) gives an expression for the SBS threshold power P_{th} as a function of the fiber parameters, SBS parameters, and scaled length.

$$P_{th} = \frac{21A\Omega_B (NA)^2}{gL_s} \tag{1.18}$$

An additional constraint on the fiber is that it must be able to accept the beam quality of the incident beam. According to ISO 11146[21], the beam quality parameter M^2 is defined

$$M^2 = \frac{\pi}{\lambda}\frac{d_o\theta}{4} \tag{1.19}$$

where d_o is the diameter of the beam waist and θ is the full beam divergence. As an approximation of the fiber parameters, let $\theta = 2NA$ and $d_o = 2a$. Since the fiber core cross-sectional area is $A = \pi a^2$, the beam quality acceptance of the fiber $M^2 \approx \pi aNA/\lambda$ can be substituted into Eq. (1.18) such that

$$P_{th} \approx \frac{21\Omega_B \lambda^2 M^4}{\pi g L_s} \tag{1.20}$$

Extrapolating the results of this work yields a relationship between L_s and the fidelity of phase conjugation. Since the experiment yielded fidelity values consistently higher than the model, a fit to the modeling data represents a lower bound to the fidelity. A linear fit to the modeled fidelity (Fig. 8) for $L_s < 40$ m·GHz is given by $F > 0.96 - (0.016\ \text{m}^{-1}\text{GHz}^{-1})L_s$. Using this relationship, the approximate SBS threshold power is a function of beam quality accepted by the fiber. Figure 9 shows three curves of the SBS threshold power as a function of the maximum M^2 accepted by the fiber which is expected to yield higher than 0.7, 0.8, and 0.9 in fidelity, with $g \approx 5\times10^{-11}$ m/W, $\lambda = 1064$ nm, and $\Omega_B = 2\pi\cdot 16$ GHz [14].

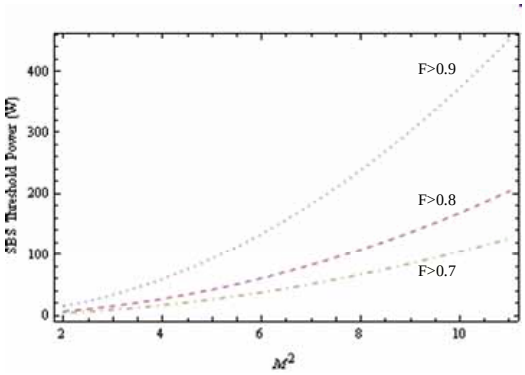

Fig. 9. SBS threshold power of a silicate fiber expected to generate a fidelity higher than 0.7, 0.8, and 0.9 as a function of the beam quality accepted by the fiber.

A reduced irradiance at an equivalent fidelity of phase conjugation can be realized when a fiber is chosen with the lowest NA possible that accepts the beam quality required. For the same M^2 value, a lower NA fiber requires a larger core area, but a longer interaction length can be used for the same fidelity. The SBS threshold power is approximately equal, and the power is spread over a larger core area in the low NA fiber. The test fibers in this work were chosen to be multimode with a low SBS threshold. Each supported nearly the same number of modes and similar beam quality (Table 1). At 40 m length, the 0.06 NA fiber reached SBS

#94567 - $15.00 USD Received 1 Apr 2008; revised 20 Jun 2008; accepted 22 Jun 2008; published 7 Jul 2008

threshold at ~14.5 W, while the 0.13 NA fiber reached threshold at ~16 W for a 15 m length. Both fibers achieved ~80% fidelity at these respective lengths, but the irradiance on the 0.06 NA fiber was reduced by a factor of four. Other fiber characteristics that effect the SBS gain coefficient such as the concentration of core dopants[22] and the SBS gain coefficient broadening with NA[23] are expected to have a secondary impact that was not included in this analysis.

5. Conclusions

High fidelity CW phase conjugation in step-index fiber is achievable with longer lengths of fiber than previously calculated. The increased fiber length reduces the SBS threshold and results in higher conversion efficiency from pump to Stokes. The specific length of fiber that can be used to generate a given phase conjugate fidelity is inversely proportional to the square of the numerical aperture of the fiber as discussed in previous works. For the same beam quality supported by the fiber, a larger core area and lower NA is preferred to generate a high fidelity phase conjugate with lower pump irradiance. This mitigates damage concerns in phase conjugate laser systems.

Acknowledgments

This work was funded in part by the High Energy Laser Joint Technology Office.

The views expressed in this article are those of the author and do not reflect the official policy or position of the United States Air Force, Department of Defense, or the U.S. Government.

#94567 - $15.00 USD Received 1 Apr 2008; revised 20 Jun 2008; accepted 22 Jun 2008; published 7 Jul 2008